



THE UNIVERSITY *of* EDINBURGH

## Edinburgh Research Explorer

# The complexity of primal-dual fixed point methods for ridge regression

### Citation for published version:

Ribeiro, AA & Richtárik, P 2018, 'The complexity of primal-dual fixed point methods for ridge regression', *Linear algebra and its applications*, vol. 556, pp. 342-372. <https://doi.org/10.1016/j.laa.2018.07.017>

### Digital Object Identifier (DOI):

[10.1016/j.laa.2018.07.017](https://doi.org/10.1016/j.laa.2018.07.017)

### Link:

[Link to publication record in Edinburgh Research Explorer](#)

### Document Version:

Publisher's PDF, also known as Version of record

### Published In:

Linear algebra and its applications

### General rights

Copyright for the publications made accessible via the Edinburgh Research Explorer is retained by the author(s) and / or other copyright owners and it is a condition of accessing these publications that users recognise and abide by the legal requirements associated with these rights.

### Take down policy

The University of Edinburgh has made every reasonable effort to ensure that Edinburgh Research Explorer content complies with UK legislation. If you believe that the public display of this file breaches copyright please contact [openaccess@ed.ac.uk](mailto:openaccess@ed.ac.uk) providing details, and we will remove access to the work immediately and investigate your claim.



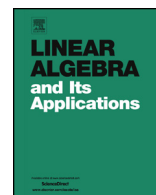


ELSEVIER

Contents lists available at ScienceDirect

# Linear Algebra and its Applications

[www.elsevier.com/locate/laa](http://www.elsevier.com/locate/laa)



## The complexity of primal-dual fixed point methods for ridge regression<sup>☆</sup>

Ademir Alves Ribeiro<sup>a,\*,1</sup>, Peter Richtárik<sup>b,2</sup>

<sup>a</sup> Department of Mathematics, Federal University of Paraná, CP 19081, 81531-980, Curitiba, PR, Brazil

<sup>b</sup> School of Mathematics, University of Edinburgh, United Kingdom

### ARTICLE INFO

#### Article history:

Received 31 August 2017

Accepted 13 July 2018

Available online 17 July 2018

Submitted by P.-A. Absil

#### MSC:

65K05

49M37

90C30

#### Keywords:

Unconstrained minimization

Primal-dual methods

Ridge regression

Fixed-point methods

### ABSTRACT

We study the ridge regression ( $L_2$  regularized least squares) problem and its dual, which is also a ridge regression problem. We observe that the optimality conditions describing the primal and dual optimal solutions can be formulated in several different but equivalent ways. The optimality conditions we identify form a linear system involving a structured matrix depending on a single relaxation parameter which we introduce for regularization purposes. This leads to the idea of studying and comparing, in theory and practice, the performance of the fixed point method applied to these reformulations. We compute the optimal relaxation parameters and uncover interesting connections between the complexity bounds of the variants of the fixed point scheme we consider. These connections follow from a close link between the spectral properties of the associated matrices. For instance, some reformulations involve purely imaginary eigenvalues; some involve real eigenvalues and others have all eigenvalues on the complex circle. We show that the deterministic Quartz method—which is a special case of the randomized dual coordinate ascent method with arbitrary sampling recently developed by Qu, Richtárik and Zhang—

<sup>☆</sup> The results of this paper were obtained between October 2014 and March 2015, during AR's affiliation with the University of Edinburgh.

\* Corresponding author.

E-mail addresses: [ademir.ribeiro@ufpr.br](mailto:ademir.ribeiro@ufpr.br) (A.A. Ribeiro), [peter.richtarik@ed.ac.uk](mailto:peter.richtarik@ed.ac.uk) (P. Richtárik).

<sup>1</sup> Supported by CNPq, Brazil, Grants 201085/2014-3 and 309437/2016-4.

<sup>2</sup> Supported by the EPSRC Grant EP/K02325X/1, “Accelerated Coordinate Descent Methods for Big Data Optimization”.

can be cast in our framework, and achieves the best rate in theory and in numerical experiments among the fixed point methods we study. Remarkably, the method achieves an accelerated convergence rate. Numerical experiments indicate that our main algorithm is competitive with the conjugate gradient method.

© 2018 Published by Elsevier Inc.

## 1. Introduction

Given matrices  $A_1, \dots, A_n \in \mathbb{R}^{d \times m}$  encoding  $n$  observations (examples), and vectors  $y_1, \dots, y_n \in \mathbb{R}^m$  encoding associated responses (labels), one is often interested in finding a vector  $w \in \mathbb{R}^d$  such that, in some precise sense, the product  $A_i^T w$  is a good approximation of  $y_i$  for all  $i$ . A fundamental approach to this problem, used in all areas of computational practice, is to formulate the problem as an  $L_2$ -regularized least-squares problem, also known as *ridge regression*. In particular, we consider the *primal* ridge regression problem

$$\min_{w \in \mathbb{R}^d} P(w) \stackrel{\text{def}}{=} \frac{1}{2n} \sum_{i=1}^n \|A_i^T w - y_i\|^2 + \frac{\lambda}{2} \|w\|^2 = \frac{1}{2n} \|A^T w - y\|^2 + \frac{\lambda}{2} \|w\|^2, \quad (1)$$

where  $\lambda > 0$  is a regularization parameter,  $\|\cdot\|$  denotes the standard Euclidean norm. In the second and more concise expression we have concatenated the observation matrices and response vectors to form a single observation matrix  $A = [A_1, A_2, \dots, A_n] \in \mathbb{R}^{d \times N}$  and a single response vector  $y = (y_1, y_2, \dots, y_n) \in \mathbb{R}^N$ , where  $N = nm$ .

With each observation  $(A_i, y_i)$  we now associate a dual variable,  $\alpha_i \in \mathbb{R}^m$ . The Fenchel *dual* of (1) is also a ridge regression problem:

$$\max_{\alpha \in \mathbb{R}^N} D(\alpha) \stackrel{\text{def}}{=} -\frac{1}{2\lambda n^2} \|A\alpha\|^2 + \frac{1}{n} \alpha^T y - \frac{1}{2n} \|\alpha\|^2, \quad (2)$$

where  $\alpha = (\alpha_1, \alpha_2, \dots, \alpha_n) \in \mathbb{R}^N$ .

**Optimality conditions.** The starting point of this work is the observation that the *optimality conditions* for the primal and dual ridge regression problems can be written in several *different* ways, in the form of a linear system involving the primal and dual variables. In particular, we find several different matrix–vector pairs  $(M, b)$ , where  $M \in \mathbb{R}^{(d+N) \times (d+N)}$  and  $b \in \mathbb{R}^{d+N}$ , such that the optimality conditions can be expressed in the form of a linear system as

$$x = Mx + b, \quad (3)$$

where  $x = (w, \alpha) \in \mathbb{R}^{d+N}$ .

**Fixed point methods.** With each system (3) one can naturally associate a fixed point method performing the iteration  $x^{k+1} = Mx^k + b$ . However, unless the spectrum of  $M$  is contained in the unit circle, such a method will not converge [1]. To overcome this drawback, we utilize the idea of *relaxation*. In particular, we pick a relaxation parameter  $\theta \neq 0$  and replace (3) with the equivalent system

$$x = G_\theta x + b_\theta,$$

where  $G_\theta = (1 - \theta)I + \theta M$  and  $b_\theta = \theta b$ . The choice  $\theta = 1$  recovers (3). We then study the convergence of the *primal-dual fixed point methods*

$$x^{k+1} = G_\theta x^k + b_\theta$$

through a careful study of the spectra of the iteration matrices  $G_\theta$ .

Our work starts with the following observation: While all these formulations are necessarily algebraically equivalent, they give rise to different fixed-point algorithms, with different convergence properties.

### 1.1. Contributions and literature review

It is well known that the role of duality in optimization and machine learning is very important, not only from the theoretical point of view but also computationally [2–4].

However, a more recent idea that has generated many contributions is the usage of the primal and dual problems together. Primal-dual methods have been employed in convex optimization problems where strong duality holds, obtaining success when applied to several types of nonlinear and nonsmooth functions that arise in various application fields, such as image processing, machine learning, inverse problems, among others [5–7].

On the other hand, fixed-point-type algorithms are classical tools for solving some structured linear systems. In particular, we have the iterative schemes developed by the mathematical economists Arrow, Hurwicz and Uzawa for solving saddle point problems [8,9].

In this paper we develop several primal-dual fixed point methods for the Ridge Regression problem. Ridge regression was introduced by Hoerl and Kennard [10,11] as a regularization method for solving least squares problems with highly correlated predictors. The goal is to reduce the standard errors of regression coefficients by imposing a penalty, in the  $L_2$  norm, on their size.

Since then, numerous papers were devoted to the study of ridge regression or even for solving problems with a general formulation in which ridge regression is a particular case. Some of these works have considered its dual formulation, proposing deterministic and stochastic algorithms that can be applied to the dual problem [12–14,2,15,4].

To the best of our knowledge, the only work that considers a primal-dual fixed point approach to deal with ridge regression is [16], where the authors deal with ill-conditioned

problems. They present an algorithm based on the gradient method and an accelerated version of this algorithm.

Here we propose methods based on the optimality conditions for the problem of minimizing the duality gap between the ridge regression problems (1) and (2) in different and equivalent ways by means of linear systems involving structured matrices. We also study the complexity of the proposed methods and prove that our main method achieves the optimal accelerated Nesterov rate. This theoretical property is supported by numerical experiments indicating that our main algorithm is competitive with the conjugate gradient method.

## 1.2. Outline

In Section 2 we formulate the optimality conditions for the problem of minimizing the duality gap between (1) and (2) in two different, but equivalent, ways by means of linear systems involving structured matrices. We also establish the duality relationship between the problems (1) and (2). In Section 3 we describe a family of (parameterized) fixed point methods applied to the reformulations for the optimality conditions. We present the convergence analysis and complexity results for these methods. Section 4 brings the main contribution of this work, with an accelerated version of the methods described in Section 3. In Section 5 we discuss some variants of our accelerated algorithm. In Section 6 we perform some numerical experiments. Finally, concluding remarks close our text in Section 7.

## 2. Separable and coupled optimality conditions

Defining  $x = (w, \alpha) \in \mathbb{R}^{d+N}$ , our primal-dual problem consists of minimizing the duality gap between the problems (1) and (2), that is

$$\min_{x \in \mathbb{R}^{d+N}} f(x) \stackrel{\text{def}}{=} P(w) - D(\alpha). \quad (4)$$

This is a quadratic strongly convex problem and therefore admits a unique global solution  $x^* \in \mathbb{R}^{d+N}$ .

### 2.1. A separable system

Note that  $\nabla f(x) = \begin{pmatrix} \nabla P(w) \\ -\nabla D(\alpha) \end{pmatrix}$ , where

$$\nabla P(w) = \frac{1}{n} A(A^T w - y) + \lambda w \quad \text{and} \quad \nabla D(\alpha) = -\frac{1}{\lambda n^2} A^T A \alpha - \frac{1}{n} \alpha + \frac{1}{n} y. \quad (5)$$

So, the first and natural way of writing the optimality conditions for problem (4) is just to set the expressions given in (5) equal to zero, which can be written as

$$\begin{pmatrix} w \\ \alpha \end{pmatrix} = -\frac{1}{\lambda n} \begin{pmatrix} AA^T & 0 \\ 0 & A^T A \end{pmatrix} \begin{pmatrix} w \\ \alpha \end{pmatrix} + \frac{1}{\lambda n} \begin{pmatrix} Ay \\ \lambda ny \end{pmatrix}. \quad (6)$$

## 2.2. A coupled system

In order to derive the duality between (1) and (2), as well as to reformulate the optimality conditions for problem (4), note that

$$P(w) = \frac{1}{n} \sum_{i=1}^n \phi_i(A_i^T w) + \lambda g(w), \quad (7)$$

where  $\phi_i(z) = \frac{1}{2}\|z - y_i\|^2$  and  $g(w) = \frac{1}{2}\|w\|^2$ .

Now, recall that the Fenchel conjugate of a convex function  $\xi : \mathbb{R}^l \rightarrow \mathbb{R}$  is  $\xi^* : \mathbb{R}^l \rightarrow \mathbb{R} \cup \{\infty\}$  defined by

$$\xi^*(u) \stackrel{\text{def}}{=} \sup_{s \in \mathbb{R}^l} \{s^T u - \xi(s)\}.$$

Note that if  $\xi$  is strongly convex, then  $\xi^*(u) < \infty$  for all  $u \in \mathbb{R}^l$ . Indeed, in this case  $\xi$  is bounded below by a strongly convex quadratic function, implying that the “sup” above is in fact a “max”.

It is easily seen that  $\phi_i^*(s) = \frac{1}{2}\|s\|^2 + s^T y_i$  and  $g^*(u) = \frac{1}{2}\|u\|^2$ . Furthermore, we have

$$D(\alpha) = -\lambda g^* \left( \frac{1}{\lambda n} \sum_{i=1}^n A_i \alpha_i \right) - \frac{1}{n} \sum_{i=1}^n \phi_i^*(-\alpha_i). \quad (8)$$

If we write

$$\bar{\alpha} \stackrel{\text{def}}{=} \frac{1}{\lambda n} A \alpha = \frac{1}{\lambda n} \sum_{i=1}^n A_i \alpha_i, \quad (9)$$

the duality gap can be written as

$$P(w) - D(\alpha) = \lambda(g(w) + g^*(\bar{\alpha}) - w^T \bar{\alpha}) + \frac{1}{n} \sum_{i=1}^n \left( \phi_i(A_i^T w) + \phi_i^*(-\alpha_i) + \alpha_i^T A_i^T w \right)$$

and the weak duality follows immediately from the fact that

$$g(w) + g^*(\bar{\alpha}) - w^T \bar{\alpha} \geq 0 \quad \text{and} \quad \phi_i(A_i^T w) + \phi_i^*(-\alpha_i) + \alpha_i^T A_i^T w \geq 0.$$

Strong duality occurs when these quantities vanish, which is precisely the same as

$$w = \nabla g^*(\bar{\alpha}) \quad \text{and} \quad \alpha_i = -\nabla \phi_i(A_i^T w)$$

or, equivalently,

$$\bar{\alpha} = \nabla g(w) \quad \text{and} \quad A_i^T w = \nabla \phi_i^*(-\alpha_i).$$

Therefore, another way to see the optimality conditions for problem (4) is by the relations

$$w = \bar{\alpha} = \frac{1}{\lambda n} A \alpha \quad \text{and} \quad \alpha = y - A^T w. \quad (10)$$

This is equivalent to

$$\boxed{\begin{pmatrix} w \\ \alpha \end{pmatrix} = -\frac{1}{\lambda n} \begin{pmatrix} 0 & -A \\ \lambda n A^T & 0 \end{pmatrix} \begin{pmatrix} w \\ \alpha \end{pmatrix} + \begin{pmatrix} 0 \\ y \end{pmatrix}.} \quad (11)$$

### 2.3. Compact form

Both reformulations of the optimality conditions, (6) and (11), can be viewed in the compact form

$$x = Mx + b, \quad (12)$$

for some  $M \in \mathbb{R}^{(d+N) \times (d+N)}$  and  $b \in \mathbb{R}^{d+N}$ . Let us denote

$$M_1 = -\frac{1}{\lambda n} \begin{pmatrix} AA^T & 0 \\ 0 & A^T A \end{pmatrix} \quad \text{and} \quad M_2 = -\frac{1}{\lambda n} \begin{pmatrix} 0 & -A \\ \lambda n A^T & 0 \end{pmatrix} \quad (13)$$

the matrices associated with the optimality conditions formulated as (6) and (11), respectively. Also, let

$$b_1 = \frac{1}{\lambda n} \begin{pmatrix} Ay \\ \lambda n y \end{pmatrix} \quad \text{and} \quad b_2 = \begin{pmatrix} 0 \\ y \end{pmatrix}. \quad (14)$$

Thus, we can rewrite (6) and (11) as

$$x = M_1 x + b_1 \quad \text{and} \quad x = M_2 x + b_2, \quad (15)$$

respectively.

### 3. Primal-dual fixed point methods

A method that arises immediately from the relation (12) is given by the scheme

$$x^{k+1} = Mx^k + b.$$

However, unless the spectrum of  $M$  is contained in the unit circle, this scheme will not converge. To overcome this drawback, we utilize the idea of *relaxation*. More precisely, we consider a relaxation parameter  $\theta \neq 0$  and replace (12) with the equivalent system

$$x = (1 - \theta)x + \theta(Mx + b).$$

Note that the choice  $\theta = 1$  recovers (12).

The proposed algorithm is then given by the following framework.

**Algorithm 3.1. Primal-Dual Fixed Point Method.**

INPUT: matrix  $M \in \mathbb{R}^{(d+N) \times (d+N)}$ , vector  $b \in \mathbb{R}^{d+N}$ , parameter  $\theta > 0$   
 STARTING POINT:  $x^0 \in \mathbb{R}^{d+N}$   
 REPEAT FOR  $k = 0, 1, 2, \dots$   
     SET  $x^{k+1} = (1 - \theta)x^k + \theta(Mx^k + b)$

As we shall see later, the use of the relaxation parameter  $\theta$  enables us to prove convergence of Algorithm 3.1 with  $M = M_1$  and  $b = b_1$  or  $M = M_2$  and  $b = b_2$ , chosen according to (13) and (14), independent of the spectral radius of these matrices.

Let us denote

$$G(\theta) = (1 - \theta)I + \theta M \quad (16)$$

and let  $x^*$  be the solution of the problem (4). Then  $x^* = Mx^* + b$  with  $M = M_1$  and  $b = b_1$  or  $M = M_2$  and  $b = b_2$ . Therefore,

$$x^* = G(\theta)x^* + \theta b.$$

Further, the iteration of Algorithm 3.1 can be written as  $x^{k+1} = G(\theta)x^k + \theta b$ . Thus,

$$\|x^k - x^*\| \leq \|G(\theta)^k\| \|x^0 - x^*\| \quad (17)$$

and consequently the convergence of the algorithm depends on the spectrum of  $G(\theta)$ . More precisely, it converges if the spectral radius of  $G(\theta)$  is less than 1, because in this case we have  $G(\theta)^k \rightarrow 0$ .

In fact, we will address the following questions:

- What is the range for  $\theta$  so that this scheme converges?
- What is the best choice of  $\theta$ ?
- What is the rate of convergence?
- How the complexity of this algorithm compares with the known ones?



### 3.1. Convergence analysis

In this section we study the convergence of Algorithm 3.1 and answer the questions raised above. To this end we point out some properties of the iteration matrices and uncover interesting connections between the complexity bounds of the variants of the fixed point scheme we consider. These connections follow from a close link between the spectral properties of the associated matrices.

For this purpose, let

$$A = U\Sigma V^T \quad (18)$$

be the singular value decomposition of  $A$ . That is,  $U \in \mathbb{R}^{d \times d}$  and  $V \in \mathbb{R}^{N \times N}$  are orthogonal matrices and

$$\Sigma = \begin{pmatrix} \tilde{\Sigma} & 0 \\ 0 & 0 \end{pmatrix} \begin{matrix} p \\ d-p \\ p & N-p \end{matrix} \quad (19)$$

where  $\tilde{\Sigma} = \text{diag}(\sigma_1, \dots, \sigma_p)$  brings the (nonzero) singular values  $\sigma_1 \geq \dots \geq \sigma_p > 0$  of  $A$ .

First, let us see a basic linear algebra result whose proof is straightforward by induction.

**Proposition 3.1.** *Let  $Q_j \in \mathbb{R}^{l \times l}$ ,  $j = 1, \dots, 4$ , be diagonal matrices whose diagonal entries are components of  $\alpha, \beta, \gamma, \delta \in \mathbb{R}^l$ , respectively. Then*

$$\det \begin{pmatrix} Q_1 & Q_2 \\ Q_3 & Q_4 \end{pmatrix} = \prod_{j=1}^l (\alpha_j \delta_j - \beta_j \gamma_j).$$

The next result is crucial for the convergence analysis and complexity study of Algorithm 3.1.

**Lemma 3.2.** *The characteristic polynomials of the matrices  $M_1$  and  $M_2$ , defined in (13), are*

$$p_1(t) = t^{N+d-2p} \prod_{j=1}^p \left( t + \frac{1}{\lambda n} \sigma_j^2 \right)^2 \quad \text{and} \quad p_2(t) = t^{N+d-2p} \prod_{j=1}^p \left( t^2 + \frac{1}{\lambda n} \sigma_j^2 \right),$$

respectively.

**Proof.** Let  $c = -\frac{1}{\lambda n}$ . From (18) and (19), we can write  $M_1 = W\Sigma_1 W^T$  and  $M_2 = W\Sigma_2 W^T$ , where  $W = \begin{pmatrix} U & 0 \\ 0 & V \end{pmatrix}$ ,  $\Sigma_1 = \begin{pmatrix} c\Sigma\Sigma^T & 0 \\ 0 & c\Sigma^T\Sigma \end{pmatrix}$  and

$$\Sigma_2 = \begin{pmatrix} 0 & 0 & -c\tilde{\Sigma} & 0 \\ 0 & 0 & 0 & 0 \\ -\tilde{\Sigma} & 0 & 0 & 0 \\ 0 & 0 & 0 & 0 \end{pmatrix} \begin{matrix} p \\ d-p \\ p \\ N-p \end{matrix}$$

$$p \quad d-p \quad p \quad N-p$$

The evaluation of  $p_1(t) = \det(tI - M_1) = \det(tI - \Sigma_1)$  is straightforward and

$$p_2(t) = \det(tI - M_2) = \det \begin{pmatrix} tI & 0 & c\tilde{\Sigma} & 0 \\ 0 & tI & 0 & 0 \\ \tilde{\Sigma} & 0 & tI & 0 \\ 0 & 0 & 0 & tI \end{pmatrix} = \det \begin{pmatrix} tI & c\tilde{\Sigma} & 0 & 0 \\ \tilde{\Sigma} & tI & 0 & 0 \\ 0 & 0 & tI & 0 \\ 0 & 0 & 0 & tI \end{pmatrix}.$$

The result then follows from Proposition 3.1.  $\square$

The following result follows directly from Lemma 3.2 and the fact that  $M_1$  is symmetric.

**Corollary 3.3.** *The spectral radii of  $M_1$  and  $M_2$  are, respectively,*

$$\rho_1 = \|M_1\| = \frac{\sigma_1^2}{\lambda n} = \frac{\|A\|^2}{\lambda n} \quad \text{and} \quad \rho_2 = \frac{\sigma_1}{\sqrt{\lambda n}} = \frac{\|A\|}{\sqrt{\lambda n}}.$$

From Corollary 3.3 we conclude that if  $\sigma_1 < \sqrt{\lambda n}$ , then  $\rho_1 \leq \rho_2 < 1$ . So,  $M_1^k \rightarrow 0$  and  $M_2^k \rightarrow 0$ , which in turn implies that the pure fixed point method, that is, Algorithm 3.1 with  $\theta = 1$ , converges. However, if  $\sigma_1 \geq \sqrt{\lambda n}$ , we cannot guarantee convergence of the pure method.

Now we shall see that Algorithm 3.1 converges for a broad range of the parameter  $\theta$ , without any assumption on  $\sigma_1$ ,  $\lambda$  or  $n$ . We begin with the analysis of the framework that uses  $M_1$  and  $b_1$ , defined in (13) and (14).

### 3.2. Fixed Point Method based on $M_1$

**Algorithm 3.2. Primal-Dual Fixed Point Method;  $M = M_1$ .**

INPUT:  $M = M_1$ ,  $b = b_1$ , parameter  $\theta > 0$

STARTING POINT:  $x^0 \in \mathbb{R}^{d+N}$

REPEAT FOR  $k = 0, 1, 2, \dots$

SET  $x^{k+1} = (1 - \theta)x^k + \theta(Mx^k + b)$

**Theorem 3.4.** *Let  $x^0 \in \mathbb{R}^{d+N}$  be an arbitrary starting point and consider the sequence  $(x^k)_{k \in \mathbb{N}}$  generated by Algorithm 3.2 with  $\theta \in \left(0, \frac{2\lambda n}{\lambda n + \sigma_1^2}\right)$ . Then the sequence  $(x^k)$*

converges to the (unique) solution of the problem (4) at a linear rate of  $\rho_1(\theta) \stackrel{\text{def}}{=} \max \left\{ \left| 1 - \theta \left( 1 + \frac{\sigma_1^2}{\lambda n} \right) \right|, 1 - \theta \right\}$ . Furthermore, if we choose  $\theta_1^* \stackrel{\text{def}}{=} \frac{2\lambda n}{2\lambda n + \sigma_1^2}$ , then the (theoretical) convergence rate is optimal and it is equal to  $\rho_1^* \stackrel{\text{def}}{=} \frac{\sigma_1^2}{2\lambda n + \sigma_1^2} = 1 - \theta_1^*$ .

**Proof.** We claim that the spectral radius of  $G_1(\theta) \stackrel{\text{def}}{=} (1 - \theta)I + \theta M_1$  is  $\rho_1(\theta)$  and also coincides with  $\|G_1(\theta)\|$ . Using Lemma 3.2, we conclude that the eigenvalues of this matrix are

$$\left\{ 1 - \theta - \frac{\theta \sigma_j^2}{\lambda n}, \quad j = 1, \dots, p \right\} \cup \{1 - \theta\}.$$

So, its spectral radius is

$$\max \left\{ \left| 1 - \theta \left( 1 + \frac{\sigma_1^2}{\lambda n} \right) \right|, 1 - \theta \right\} = \rho_1(\theta).$$

Since  $G_1(\theta)$  is symmetric, this quantity coincides with  $\|G_1(\theta)\|$ . Furthermore, the admissible values for  $\theta$ , that is, the ones such that the eigenvalues have modulus less than one, can be found by solving

$$\left| 1 - \theta \left( 1 + \frac{\sigma_1^2}{\lambda n} \right) \right| < 1,$$

which immediately gives  $0 < \theta < \frac{2\lambda n}{\lambda n + \sigma_1^2}$ . So, the linear convergence of Algorithm 3.1 is guaranteed for any  $\theta \in \left( 0, \frac{2\lambda n}{\lambda n + \sigma_1^2} \right)$ . Finally, note that the solution of the problem

$$\min_{\theta > 0} \rho_1(\theta)$$

is achieved when  $\theta \left( 1 + \frac{\sigma_1^2}{\lambda n} \right) - 1 = 1 - \theta$ , yielding  $\theta_1^* = \frac{2\lambda n}{2\lambda n + \sigma_1^2}$  and the optimal convergence rate  $\rho_1^* = \frac{\sigma_1^2}{2\lambda n + \sigma_1^2}$ .  $\square$

The top picture of Fig. 1 illustrates the eigenvalues of  $G_1(\theta)$  (magenta squares) together with the eigenvalues of  $M_1$  (blue triangles), for a fixed value of the parameter  $\theta$ . The one farthest from the origin is  $1 - \theta - \frac{\theta \sigma_1^2}{\lambda n}$  or  $1 - \theta$ . On the bottom we show the two largest (in absolute value) eigenvalues of  $G_1(\theta)$  corresponding to the optimal choice of  $\theta$ .

Now we analyze the fixed point framework that employs  $M_2$  and  $b_2$ , defined in (13) and (14).

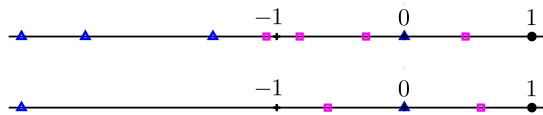


**Fig. 1.** Eigenvalues of  $G_1(\theta)$  (magenta squares) and  $M_1$  (blue triangles). (For interpretation of the colors in the figure(s), the reader is referred to the web version of this article.)

### 3.3. Fixed Point Method based on $M_2$

**Algorithm 3.3. Primal-Dual Fixed Point Method;  $M = M_2$ .**

INPUT:  $M = M_2$ ,  $b = b_2$ , parameter  $\theta > 0$

STARTING POINT:  $x^0 \in \mathbb{R}^{d+N}$

REPEAT FOR  $k = 0, 1, 2, \dots$

SET  $x^{k+1} = (1 - \theta)x^k + \theta(Mx^k + b)$

**Theorem 3.5.** Let  $x^0 \in \mathbb{R}^{d+N}$  be an arbitrary starting point and consider the sequence  $(x^k)_{k \in \mathbb{N}}$  generated by Algorithm 3.3 with  $\theta \in \left(0, \frac{2\lambda n}{\lambda n + \sigma_1^2}\right)$ . Then the sequence  $(x^k)$  converges to the (unique) solution of the problem (4) at an asymptotic convergence rate of  $\rho_2(\theta) \stackrel{\text{def}}{=} \sqrt{(1 - \theta)^2 + \frac{\theta^2 \sigma_1^2}{\lambda n}}$ . Furthermore, if we choose  $\theta_2^* \stackrel{\text{def}}{=} \frac{\lambda n}{\lambda n + \sigma_1^2}$ , then the (theoretical) convergence rate is optimal and it is equal to  $\rho_2^* \stackrel{\text{def}}{=} \frac{\sigma_1}{\sqrt{\lambda n + \sigma_1^2}} = \sqrt{1 - \theta_2^*}$ .

**Proof.** First, using Lemma 3.2, we conclude that the eigenvalues of  $G_2(\theta) \stackrel{\text{def}}{=} (1 - \theta)I + \theta M_2$  are

$$\left\{1 - \theta \pm \frac{\theta \sigma_j}{\sqrt{\lambda n}} i, \quad j = 1, \dots, p\right\} \cup \{1 - \theta\},$$

where  $i = \sqrt{-1}$ . The two ones with largest modulus are  $1 - \theta \pm \frac{\theta \sigma_1}{\sqrt{\lambda n}} i$  (see Fig. 2). So, the spectral radius of  $G_2(\theta)$  is

$$\sqrt{(1 - \theta)^2 + \frac{\theta^2 \sigma_1^2}{\lambda n}} = \rho_2(\theta).$$

Further, the values of  $\theta$  for which the eigenvalues of  $G_2(\theta)$  have modulus less than one can be found by solving  $(1 - \theta)^2 + \frac{\theta^2 \sigma_1^2}{\lambda n} < 1$  giving

$$0 < \theta < \frac{2\lambda n}{\lambda n + \sigma_1^2}.$$

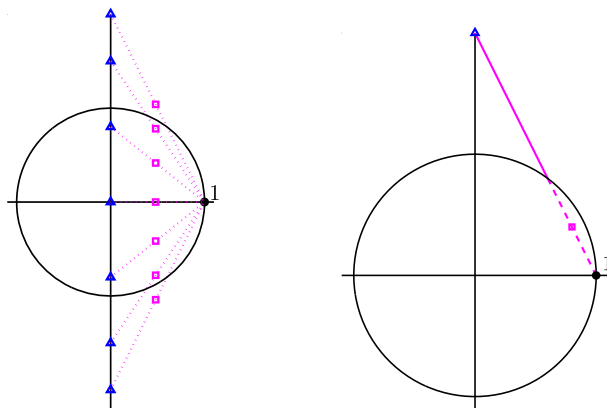


Fig. 2. Eigenvalues of  $G_2(\theta)$  (magenta squares) and  $M_2$  (blue triangles), represented in the complex plane.

The asymptotic convergence follows from the fact that  $\|G_2(\theta)^k\|^{1/k} \rightarrow \rho_2(\theta)$ . Indeed, using (17) we conclude that

$$\left( \frac{\|x^k - x^*\|}{\|x^0 - x^*\|} \right)^{1/k} \leq \|G_2(\theta)^k\|^{1/k} \rightarrow \rho_2(\theta).$$

This means that given  $\gamma > 0$ , there exists  $k_0 \in \mathbb{N}$  such that

$$\|x^k - x^*\| \leq (\rho_2(\theta) + \gamma)^k \|x^0 - x^*\|$$

for all  $k \geq k_0$ . Finally, the optimal parameter  $\theta_2^*$  and the corresponding optimal rate  $\rho_2^*$  can be obtained directly by solving

$$\min_{\theta > 0} (1 - \theta)^2 + \frac{\theta^2 \sigma_1^2}{\lambda n}. \quad \square$$

The left picture of Fig. 2 illustrates, in the complex plane, the eigenvalues of  $G_2(\theta)$  (magenta squares) together with the eigenvalues of  $M_2$  (blue triangles), for a fixed value of the parameter  $\theta$ . On the right we show, for each  $\theta \in (0, 1)$ , one of the two eigenvalues of  $G_2(\theta)$  farthest from the origin. The dashed segment corresponds to the admissible values for  $\theta$ , that is, the eigenvalues with modulus less than one. The square corresponds to the optimal choice of  $\theta$ .

### 3.4. Comparison of the rates

We summarize the discussion above in Table 1 which brings the comparison between the pure ( $\theta = 1$ ) and optimal ( $\theta = \theta_j^*$ ,  $j = 1, 2$ ) versions of Algorithm 3.1. We can see that the convergence rate of the optimal version is  $\frac{\lambda n}{2\lambda n + \sigma_1^2}$  times the one of the

**Table 1**  
Ranges of convergence and convergence rates of pure and optimal versions of Algorithm 3.2 (the one that uses  $M_1$ ), indicated by PDFP1( $\theta$ ), and Algorithm 3.3 (the one that uses  $M_2$ ), PDFP2( $\theta$ ).

	PDFP1( $\theta$ )	PDFP2( $\theta$ )
Range of $\theta$	$\left(0, \frac{2\lambda n}{\lambda n + \sigma_1^2}\right)$	$\left(0, \frac{2\lambda n}{\lambda n + \sigma_1^2}\right)$
Pure ( $\theta = 1$ )	$\frac{\sigma_1^2}{\lambda n}$	$\frac{\sigma_1}{\sqrt{\lambda n}}$
Optimal ( $\theta = \theta_j^*$ )	$\frac{\sigma_1^2}{2\lambda n + \sigma_1^2} = 1 - \theta_1^*$	$\sqrt{\frac{\sigma_1^2}{\lambda n + \sigma_1^2}} = \sqrt{1 - \theta_2^*}$

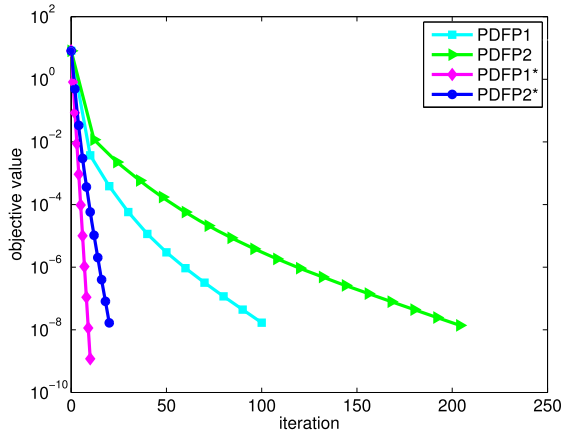


**Fig. 3.** Performance of pure and optimal versions of Algorithms 3.2 and 3.3 applied to solve the problem (4). The picture shows the objective values against the number of iterations. The dimensions considered were  $d = 200$ ,  $m = 1$  and  $n = 5000$  (so that the total dimension is  $d + N = d + nm = 5200$ ). The matrix  $A \in \mathbb{R}^{d \times N}$  and the vector  $y \in \mathbb{R}^N$  were randomly generated. For simplicity of notation we have denoted the pure and optimal versions of Algorithm 3.2 by PDFP1 and PDFP1\*, respectively. Analogously, for Algorithm 3.3, we used PDFP2 and PDFP2\* to denote the pure and optimal versions, respectively. In order to keep the figure legible, we plotted a square every 10 iterations for PDFP1, a triangle every 12 iterations for PDFP2, a diamond per iteration for PDFP1\* and a circle every 2 iterations for PDFP2\*.

pure version if  $M_1$  is employed (Algorithm 3.2) and  $\sqrt{\frac{\lambda n}{\lambda n + \sigma_1^2}}$  times the pure version when using  $M_2$  (Algorithm 3.3). Moreover, in any case, employing  $M_1$  provides faster convergence. This can be seen in Fig. 3, where Algorithm 3.1 was applied to solve the problem (4). The dimensions considered were  $d = 200$ ,  $m = 1$  and  $n = 5000$  (so that the total dimension is  $d + N = d + nm = 5200$ ).

We also mention that the pure version does not require the knowledge of  $\sigma_1$ , but it may not converge. On the other hand, the optimal version always converges, but  $\theta$  depends on  $\sigma_1$ .

### 3.5. Direct relationship between the iterates of the two methods

Another relation regarding the employment of  $M_1$  or  $M_2$  in the pure version of Algorithm 3.1, which is also illustrated in Fig. 3, is that one step of the method with  $M_1$  corresponds exactly to two steps of the one with  $M_2$ . Indeed, note first that  $M_2^2 = M_1$ . Thus, denoting the current point by  $x$  and the next iterate by  $x_M^+$ , in view of (15) we have

$$\begin{aligned} x_{M_2}^{++} &= M_2 x_{M_2}^+ + b_2 \\ &= M_2(M_2 x + b_2) + b_2 \\ &= M_1 x + M_2 b_2 + b_2 \\ &= M_1 x + b_1 \\ &= x_{M_1}^+. \end{aligned}$$

In Section 4 we shall see how this behavior can invert with a small change in the computation of the dual variable.

### 3.6. Complexity results

In order to establish the complexity of Algorithm 3.1 we need to calculate the condition number of the objective function, defined in (4). Note that the Hessian of  $f$  is given by

$$\nabla^2 f = \frac{1}{n} \begin{pmatrix} AA^T + \lambda n I & 0 \\ 0 & \frac{1}{\lambda n} A^T A + I \end{pmatrix}$$

Let us consider two cases:

- If  $\lambda n \geq 1$ , then  $\sigma_1^2 + \lambda n \geq \sigma_1^2 + 1 \geq \frac{\sigma_1^2}{\lambda n} + 1$ , which in turn implies that the largest eigenvalue of  $\nabla^2 f$  is  $L = \frac{\sigma_1^2 + \lambda n}{n}$ . The smallest eigenvalue is

$$\begin{cases} \frac{1}{n}, & \text{if } d < N \\ \frac{\sigma_d^2}{\lambda n^2} + \frac{1}{n}, & \text{if } d = N \\ \min \left\{ \lambda, \frac{\sigma_N^2}{\lambda n^2} + \frac{1}{n} \right\}, & \text{if } d > N. \end{cases}$$

Therefore, if  $d < N$ , the condition number of  $\nabla^2 f$  is the condition number of  $\nabla^2 f$  is

$$\sigma_1^2 + \lambda n. \quad (20)$$

- If  $\lambda n < 1$ , then  $\sigma_1^2 + \lambda n < \sigma_1^2 + 1 < \frac{\sigma_1^2}{\lambda n} + 1$ , which in turn implies that the largest eigenvalue of  $\nabla^2 f$  is  $L = \frac{\sigma_1^2 + \lambda n}{\lambda n^2}$ . The smallest eigenvalue is

$$\begin{cases} \min \left\{ \frac{\sigma_d^2}{n} + \lambda, \frac{1}{n} \right\}, & \text{if } d < N \\ \frac{\sigma_d^2}{n} + \lambda, & \text{if } d = N \\ \lambda, & \text{if } d > N. \end{cases}$$

So, assuming that  $d < N$ , the condition number is  $\frac{\sigma_1^2 + \lambda n}{\lambda n^2 \min \left\{ \frac{\sigma_d^2}{n} + \lambda, \frac{1}{n} \right\}}$ . If  $A$  is rank deficient, then the condition number is

$$\frac{\sigma_1^2 + \lambda n}{(\lambda n)^2}. \quad (21)$$

We stress that despite the analysis was made in terms of the sequence  $x^k = (w^k, \alpha^k)$ , the linear convergence also applies to objective values. Indeed, since  $f$  is  $L$ -smooth, we have

$$f(x^k) \leq f(x^*) + \nabla f(x^*)^T (x^k - x^*) + \frac{L}{2} \|x^k - x^*\|^2 = \frac{L}{2} \|x^k - x^*\|^2,$$

where the equality follows from the fact that the optimal objective value is zero. Therefore, if we want to get  $f(x^k) - f(x^*) < \varepsilon$  and we have linear convergence rate  $\rho$  on the sequence  $(x^k)$ , then it is enough to enforce

$$\frac{L}{2} \rho^{2k} \|x^0 - x^*\|^2 < \varepsilon,$$

or equivalently,

$$k > \frac{-1}{2 \log \rho} \log \left( \frac{\|x^0 - x^*\|^2 L}{2\varepsilon} \right). \quad (22)$$

Using the estimate  $\log(1 - \theta) \approx -\theta$ , we can approximate the right hand side of (22) by

$$\frac{1}{2\theta_1^*} \log \left( \frac{\|x^0 - x^*\|^2 L}{2\varepsilon} \right), \quad (23)$$

in the case  $M_1$  is used and by



$$\frac{1}{\theta_2^*} \log \left( \frac{\|x^0 - x^*\|^2 L}{2\varepsilon} \right), \quad (24)$$

if we use  $M_2$ .

In order to estimate the above expressions in terms of the condition number, let us consider the more common case  $\lambda n \geq 1$ . Then the condition number of  $\nabla^2 f$  is given by (20), that is,

$$\kappa \stackrel{\text{def}}{=} \sigma_1^2 + \lambda n. \quad (25)$$

So, if we use  $M_1$ , the complexity is proportional to

$$\frac{1}{2\theta_1^*} = \frac{\sigma_1^2 + 2\lambda n}{4\lambda n} = \frac{\kappa + \lambda n}{4\lambda n}. \quad (26)$$

If we use  $M_2$ , the complexity is proportional to

$$\frac{1}{\theta_2^*} = \frac{\lambda n + \sigma_1^2}{\lambda n} = \frac{\kappa}{\lambda n}. \quad (27)$$

#### 4. Accelerated Primal-Dual Fixed Point Method

Now we present our main contribution. When we employ Algorithm 3.3, the primal and dual variables are mixed in two equations. More precisely, in view of (9) the iteration in this case can be rewritten as

$$\begin{cases} w^{k+1} = (1 - \theta)w^k + \theta\bar{\alpha}^k \\ \alpha^{k+1} = (1 - \theta)\alpha^k + \theta(y - A^T w^k). \end{cases}$$

The idea here is to apply block Gauss–Seidel to this system. That is, we use the freshest  $w$  to update  $\alpha$ . Let us state formally the method by means of the following framework.

##### Algorithm 4.1. Accelerated Fixed Point Method.

INPUT: matrix  $A \in \mathbb{R}^{d \times N}$ , vector  $y \in \mathbb{R}^N$ , parameter  $\theta \in (0, 1]$   
 STARTING POINTS:  $w^0 \in \mathbb{R}^d$  and  $\alpha^0 \in \mathbb{R}^N$   
 REPEAT FOR  $k = 0, 1, 2, \dots$   
     SET  $w^{k+1} = (1 - \theta)w^k + \theta\bar{\alpha}^k$   
     SET  $\alpha^{k+1} = (1 - \theta)\alpha^k + \theta(y - A^T w^{k+1})$

Due to this modification, we can achieve faster convergence. This algorithm is a deterministic version of a randomized primal-dual algorithm (Quartz) proposed and analyzed by Qu, Richtárik and Zhang [7].

#### 4.1. Convergence analysis

In this section we study the convergence of Algorithm 4.1. We shall determine all values for the parameter  $\theta$  for which this algorithm converges as well as the one giving the best convergence rate.

To this end, we start by showing that Algorithm 4.1 can be viewed as a fixed point scheme. Then we determine the “dynamic” spectral properties of the associated matrices, which are parameterized by  $\theta$ .

First, note that the iteration of our algorithm can be written as

$$\begin{pmatrix} I & 0 \\ \theta A^T & I \end{pmatrix} \begin{pmatrix} w^{k+1} \\ \alpha^{k+1} \end{pmatrix} = \begin{pmatrix} (1-\theta)I & \frac{\theta}{\lambda n} A \\ 0 & (1-\theta)I \end{pmatrix} \begin{pmatrix} w^k \\ \alpha^k \end{pmatrix} + \begin{pmatrix} 0 \\ \theta y \end{pmatrix}$$

or in a compact way as

$$x^{k+1} = G_3(\theta)x^k + f \quad (28)$$

with

$$G_3(\theta) = (1-\theta)I + \theta \begin{pmatrix} 0 & \frac{1}{\lambda n} A \\ (\theta-1)A^T & -\frac{\theta}{\lambda n} A^T A \end{pmatrix} \quad (29)$$

and  $f = \begin{pmatrix} 0 \\ \theta y \end{pmatrix}$ .

We know that if the spectral radius of  $G_3(\theta)$  is less than 1, then the sequence defined by (28) converges. Indeed, in this case the limit point is just  $x^*$ , the solution of the problem (4). This follows from the fact that  $x^* = G_3(\theta)x^* + f$ .

Next lemma provides the spectrum of  $G_3(\theta)$ .

**Lemma 4.1.** *The eigenvalues of the matrix  $G_3(\theta)$ , defined in (29), are given by*

$$\frac{1}{2\lambda n} \left\{ 2(1-\theta)\lambda n - \theta^2 \sigma_j^2 \pm \theta \sigma_j \sqrt{\theta^2 \sigma_j^2 - 4(1-\theta)\lambda n} \right\} \cup \{1-\theta\}, \quad j = 1, \dots, p$$

**Proof.** Consider the matrix  $M_3(\theta) \stackrel{\text{def}}{=} \begin{pmatrix} 0 & \frac{1}{\lambda n} A \\ (\theta-1)A^T & -\frac{\theta}{\lambda n} A^T A \end{pmatrix}$ . Using the singular value decomposition of  $A$ , given in (18), we can write

$$M_3(\theta) = \begin{pmatrix} U & 0 \\ 0 & V \end{pmatrix} \begin{pmatrix} 0 & \frac{1}{\lambda n} \Sigma \\ (\theta-1)\Sigma^T & -\frac{\theta}{\lambda n} \Sigma^T \Sigma \end{pmatrix} \begin{pmatrix} U^T & 0 \\ 0 & V^T \end{pmatrix}.$$

Therefore, the eigenvalues of  $M_3(\theta)$  are the same as the ones of

$$\begin{pmatrix} 0 & \frac{1}{\lambda n} \Sigma \\ (\theta - 1) \Sigma^T & -\frac{\theta}{\lambda n} \Sigma^T \Sigma \end{pmatrix} = \begin{pmatrix} 0 & 0 & -c \tilde{\Sigma} & 0 \\ 0 & 0 & 0 & 0 \\ (\theta - 1) \tilde{\Sigma} & 0 & \theta c \tilde{\Sigma}^2 & 0 \\ 0 & 0 & 0 & 0 \end{pmatrix} \begin{matrix} p \\ d - p \\ p \\ N - p \end{matrix}$$

$p \qquad d - p \qquad p \qquad N - p$

where  $c = -\frac{1}{\lambda n}$  and  $\tilde{\Sigma}$  is defined in (19). The characteristic polynomial of this matrix is

$$\begin{aligned} p_\theta(t) &= \det \begin{pmatrix} tI & 0 & c \tilde{\Sigma} & 0 \\ 0 & tI & 0 & 0 \\ (1 - \theta) \tilde{\Sigma} & 0 & tI - \theta c \tilde{\Sigma}^2 & 0 \\ 0 & 0 & 0 & tI \end{pmatrix} \\ &= \det \begin{pmatrix} tI & c \tilde{\Sigma} & 0 & 0 \\ (1 - \theta) \tilde{\Sigma} & tI - \theta c \tilde{\Sigma}^2 & 0 & 0 \\ 0 & 0 & tI & 0 \\ 0 & 0 & 0 & tI \end{pmatrix}. \end{aligned}$$

Using Proposition 3.1 and denoting  $q = N + d - 2p$ , we obtain

$$p_\theta(t) = t^q \prod_{j=1}^p \left( t(t - \theta c \sigma_j^2) - c(1 - \theta) \sigma_j^2 \right) = t^q \prod_{j=1}^p \left( t^2 + \frac{\theta \sigma_j^2}{\lambda n} t + \frac{(1 - \theta) \sigma_j^2}{\lambda n} \right).$$

Thus, the eigenvalues of  $M_3(\theta)$  are

$$\frac{1}{2\lambda n} \left\{ -\theta \sigma_j^2 \pm \sigma_j \sqrt{\theta^2 \sigma_j^2 - 4(1 - \theta) \lambda n}, \quad j = 1, \dots, p \right\} \cup \{0\},$$

so that the eigenvalues of  $G_3(\theta) = (1 - \theta)I + \theta M_3(\theta)$  are

$$\frac{1}{2\lambda n} \left\{ 2(1 - \theta) \lambda n - \theta^2 \sigma_j^2 \pm \theta \sigma_j \sqrt{\theta^2 \sigma_j^2 - 4(1 - \theta) \lambda n}, \quad j = 1, \dots, p \right\} \cup \{1 - \theta\},$$

giving the desired result.  $\square$

Fig. 4 illustrates, in the complex plane, the spectrum of the matrix  $G_3(\theta)$  for many different values of  $\theta$ . We used  $n = 250$ ,  $d = 13$ ,  $m = 1$  (therefore  $N = 250$ ),  $\lambda = 0.3$  and a random matrix  $A \in \mathbb{R}^{d \times N}$ . The pictures point out the fact that for some range of  $\theta$  the spectrum is contained in a circle and for other values of  $\theta$  some of the eigenvalues remain in a circle while others are distributed along the real line, moving monotonically as this parameter changes. These statements will be proved in the sequel.

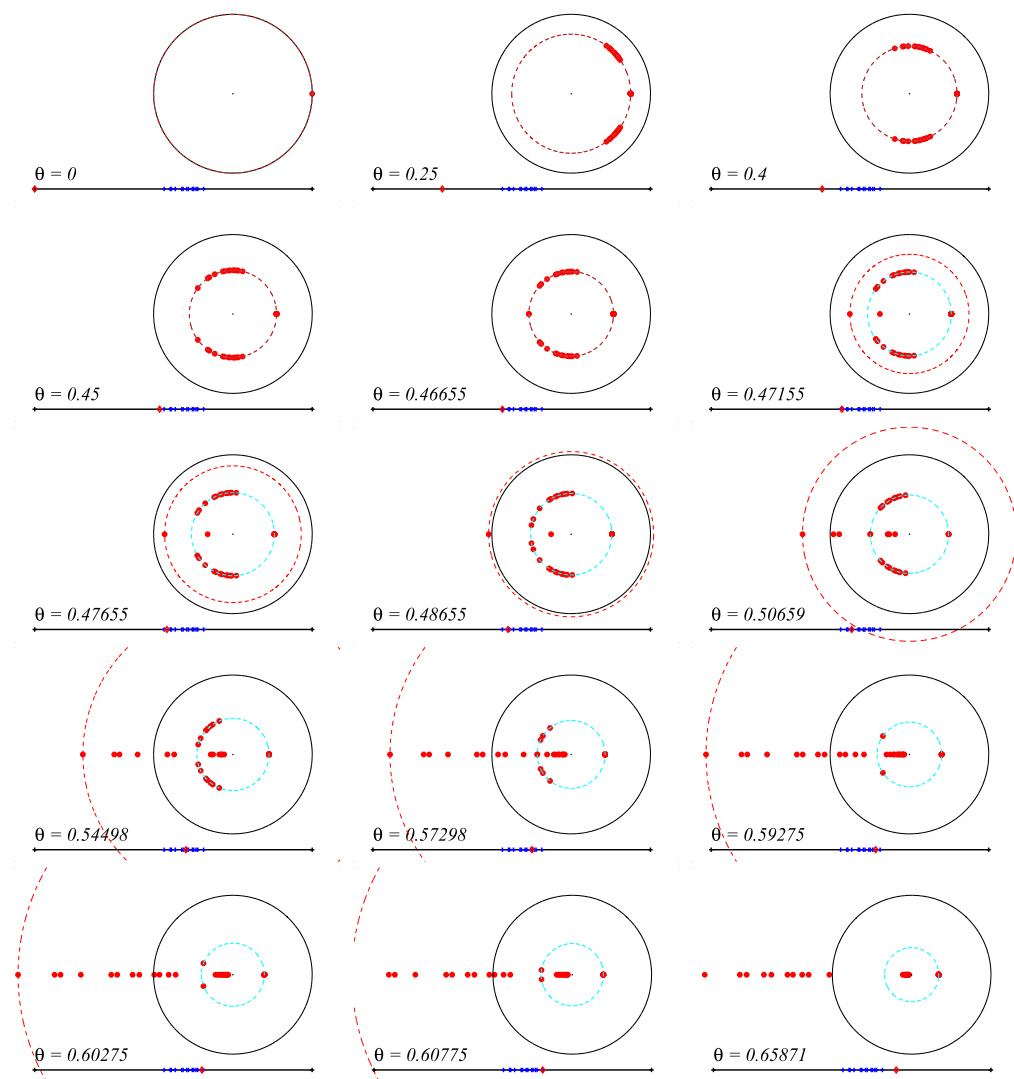


**Fig. 4.** The spectrum of  $G_3(\theta)$  for many different values of  $\theta$ . The first 4 pictures satisfying the condition  $\theta^2\sigma_1^2 - 4(1-\theta)\lambda n < 0$ ; in the fifth picture we have  $\theta^2\sigma_1^2 - 4(1-\theta)\lambda n = 0$  and the remaining ones represent the case where  $\theta^2\sigma_1^2 - 4(1-\theta)\lambda n > 0$ . The straight line represents (in a different scale) the interval  $[0, 1]$  on which are plotted some specific values of  $\theta$  (blue marks), defined in (31). The red diamond corresponds to the current value of  $\theta$ .

In what follows, let us consider the functions  $\delta_j : [0, 1] \rightarrow \mathbb{R}$  defined by

$$\delta_j(\theta) = \theta^2\sigma_j^2 - 4(1-\theta)\lambda n. \quad (30)$$

The following straightforward result brings some basic properties of them, illustrated in Fig. 5.

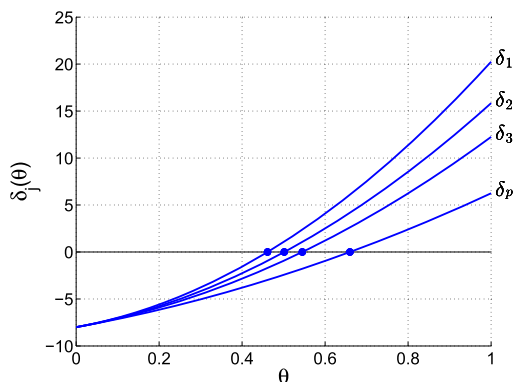


Fig. 5. The functions  $\delta_j$ ,  $j = 1, \dots, p$  and the properties stated in Lemma 4.2.

**Lemma 4.2.** Each function  $\delta_j$ ,  $j = 1, \dots, p$ , is strictly increasing, from  $-4\lambda n$  to  $\sigma_j^2$  as  $\theta$  goes from zero to 1. Furthermore, these functions are sorted in decreasing order,  $\delta_1 \geq \delta_2 \geq \dots \geq \delta_p$ , and their zeros,

$$\bar{\theta}_j \stackrel{\text{def}}{=} \frac{-2\lambda n + 2\sqrt{\lambda n(\lambda n + \sigma_j^2)}}{\sigma_j^2}, \quad (31)$$

are sorted in increasing order:  $0 < \bar{\theta}_1 \leq \bar{\theta}_2 \leq \dots \leq \bar{\theta}_p < 1$ .

Now we shall study the spectrum of  $G_3(\theta)$ , given in Lemma 4.1. For this, let us denote

$$\lambda_0(\theta) \stackrel{\text{def}}{=} (1 - \theta) \quad (32)$$

and, for  $j = 1, \dots, p$ ,

$$\lambda_j^-(\theta) \stackrel{\text{def}}{=} \frac{1}{2\lambda n} \left( 2(1 - \theta)\lambda n - \theta^2 \sigma_j^2 - \theta \sigma_j \sqrt{\delta_j(\theta)} \right), \quad (33)$$

$$\lambda_j^+(\theta) \stackrel{\text{def}}{=} \frac{1}{2\lambda n} \left( 2(1 - \theta)\lambda n - \theta^2 \sigma_j^2 + \theta \sigma_j \sqrt{\delta_j(\theta)} \right) \quad (34)$$

where  $\delta_j$  is defined in (30).

**Lemma 4.3.** Consider  $\bar{\theta}_1$  as defined in (31). If  $\theta \in [0, \bar{\theta}_1]$ , then

$$|\lambda_j^+(\theta)| = |\lambda_j^-(\theta)| = 1 - \theta$$

for all  $j = 1, \dots, p$ , which in turn implies that the spectral radius of  $G_3(\theta)$  is  $1 - \theta$ .

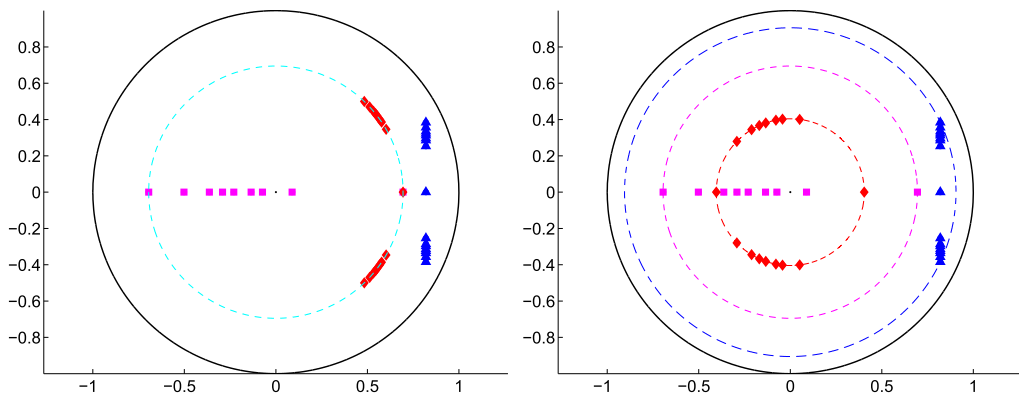


**Fig. 6.** On the left, the spectrum of  $G_1(\theta_1^*)$  (magenta squares),  $G_2(\theta_2^*)$  (blue triangles) and  $G_3(\theta_1^*)$  (red diamonds). On the right, the spectrum of  $G_3(\theta_3^*)$ , where  $\theta_3^*$  is the optimal parameter.

**Proof.** Note that in this case we have  $\delta_j(\theta) \leq 0$  for all  $j = 1, \dots, p$ . So,

$$\begin{aligned} |\lambda_j^+(\theta)|^2 &= |\lambda_j^-(\theta)|^2 \\ &= \frac{1}{4\lambda^2 n^2} \left( \left( 2(1-\theta)\lambda n - \theta^2 \sigma_j^2 \right)^2 - \theta^2 \sigma_j^2 \delta_j(\theta) \right) \\ &= (1-\theta)^2, \end{aligned}$$

yielding the desired result since  $\theta \leq 1$ .  $\square$

It can be shown that the parameter  $\theta = \theta_1^*$ , defined in Theorem 3.4, satisfies the conditions of Lemma 4.3. So, the spectral radius of  $G_3(\theta_1^*)$  is  $1 - \theta_1^*$ , exactly the same spectral radius of  $G_1(\theta_1^*) = (1 - \theta_1^*)I + \theta_1^*M_1$ . This is shown in Fig. 6, together with the spectrum of  $G_2(\theta_2^*) = (1 - \theta_2^*)I + \theta_2^*M_2$ . We also show in this figure (the right picture) the spectrum of  $G_3(\theta_3^*)$ , where  $\theta_3^*$  is the optimal parameter. This parameter will be determined later, in Theorem 4.6.

**Lemma 4.4.** Consider  $\bar{\theta}_j$ ,  $j = 1, \dots, p$ , as defined in (31). If  $\theta \in [\bar{\theta}_l, \bar{\theta}_{l+1}]$ , then the eigenvalues  $\lambda_j^+(\theta)$  and  $\lambda_j^-(\theta)$ ,  $j = 1, \dots, l$ , are real numbers satisfying

$$\lambda_1^-(\theta) \leq \dots \leq \lambda_l^-(\theta) \leq \theta - 1 \leq \lambda_l^+(\theta) \leq \dots \leq \lambda_1^+(\theta) \leq 0.$$

On the other hand, for  $j = l + 1, \dots, p$  we have

$$|\lambda_j^+(\theta)| = |\lambda_j^-(\theta)| = 1 - \theta$$

Thus, the spectral radius of  $G_3(\theta)$  is  $-\lambda_1^-(\theta)$ .

**Proof.** We have  $\delta_j(\theta) \geq 0$  for all  $j = 1, \dots, l$ . So,

$$\begin{aligned}\lambda_j^+(\theta) - (\theta - 1) &= \frac{1}{2\lambda n} \left( 2(1 - \theta)\lambda n - \theta^2\sigma_j^2 + \theta\sigma_j\sqrt{\delta_j(\theta)} \right) + 1 - \theta \\ &= \frac{1}{2\lambda n} \left( 4(1 - \theta)\lambda n - \theta^2\sigma_j^2 + \theta\sigma_j\sqrt{\delta_j(\theta)} \right) \\ &= \frac{1}{2\lambda n} \left( -\delta_j(\theta) + \theta\sigma_j\sqrt{\delta_j(\theta)} \right) \\ &= \frac{\sqrt{\delta_j(\theta)}}{2\lambda n} \left( \theta\sigma_j - \sqrt{\delta_j(\theta)} \right) \geq 0.\end{aligned}$$

Furthermore,

$$\left( \theta\sigma_j\sqrt{\delta_j(\theta)} \right)^2 = \theta^2\sigma_j^2 \left( \theta^2\sigma_j^2 - 4(1 - \theta)\lambda n \right) \leq \left( \theta^2\sigma_j^2 - 2(1 - \theta)\lambda n \right)^2.$$

Since  $\theta^2\sigma_j^2 - 2(1 - \theta)\lambda n = \delta_j(\theta) + 2(1 - \theta)\lambda n \geq 0$ ,

$$\lambda_j^+(\theta) = \frac{1}{2\lambda n} \left( 2(1 - \theta)\lambda n - \theta^2\sigma_j^2 + \theta\sigma_j\sqrt{\delta_j(\theta)} \right) \leq 0.$$

Now, note that

$$\begin{aligned}\lambda_j^-(\theta) - (\theta - 1) &= \frac{1}{2\lambda n} \left( 2(1 - \theta)\lambda n - \theta^2\sigma_j^2 - \theta\sigma_j\sqrt{\delta_j(\theta)} \right) + 1 - \theta \\ &= \frac{1}{2\lambda n} \left( -\delta_j(\theta) - \theta\sigma_j\sqrt{\delta_j(\theta)} \right) \leq 0.\end{aligned}$$

Moreover, from Lemma 4.2 and the definition of  $\sigma_j$ , we have  $\delta_1(\theta) \geq \dots \geq \delta_l(\theta)$  and  $\sigma_1 \geq \dots \geq \sigma_l$ , which imply that  $\lambda_1^-(\theta) \leq \dots \leq \lambda_l^-(\theta)$ . The inequality  $\lambda_l^+(\theta) \leq \dots \leq \lambda_1^+(\theta)$  follows from the fact that the function

$$[\sqrt{a}, \infty) \ni s \mapsto -s^2 + s\sqrt{s^2 - a}$$

is increasing. Finally, for  $j = l + 1, \dots, p$  we have  $\delta_j(\theta) \leq 0$  and, by the same argument used in Lemma 4.3, we conclude that  $|\lambda_j^+(\theta)| = |\lambda_j^-(\theta)| = 1 - \theta$ .  $\square$

From Lemmas 4.3 and 4.4 we can conclude that  $\bar{\theta}_1$  is the threshold value for  $\theta$  after which the eigenvalues of  $G_3(\theta)$  start departing the circle of radius  $1 - \theta$ . The next result presents the threshold after which the eigenvalues are all real.

**Lemma 4.5.** Consider  $\bar{\theta}_p$  as defined in (31). If  $\theta \geq \bar{\theta}_p$ , then the eigenvalues  $\lambda_j^+(\theta)$  and  $\lambda_j^-(\theta)$ ,  $j = 1, \dots, p$ , are real numbers satisfying

$$\lambda_1^-(\theta) \leq \dots \leq \lambda_p^-(\theta) \leq \theta - 1 \leq \lambda_p^+(\theta) \leq \dots \leq \lambda_1^+(\theta) \leq 0.$$

Thus, the spectral radius of  $G_3(\theta)$  is  $-\lambda_1^-(\theta)$ .

**Proof.** The same presented for Lemma 4.4.  $\square$

Using the previous results, we can finally establish the convergence of Algorithm 4.1 (Deterministic Quartz).

**Theorem 4.6.** *Let  $w^0 \in \mathbb{R}^d$  and  $\alpha^0 \in \mathbb{R}^N$  be arbitrary and consider the sequence  $(w^k, \alpha^k)_{k \in \mathbb{N}}$  generated by Algorithm 4.1 with  $\theta \in \left(0, \frac{2\sqrt{\lambda n}}{\sqrt{\lambda n} + \sigma_1}\right)$ . Then the sequence  $(w^k, \alpha^k)$  converges to the (unique) solution of the problem (4) at an asymptotic linear rate of*

$$\rho_3(\theta) \stackrel{\text{def}}{=} \begin{cases} 1 - \theta, & \text{if } \theta \in (0, \bar{\theta}_1] \\ \frac{1}{2\lambda n} \left( \theta \sigma_1 \sqrt{\delta_1(\theta)} + \theta^2 \sigma_1^2 - 2(1 - \theta)\lambda n \right), & \text{if } \theta \geq \bar{\theta}_1, \end{cases}$$

where  $\bar{\theta}_1 = \frac{-2\lambda n + 2\sqrt{\lambda n(\lambda n + \sigma_1^2)}}{\sigma_1^2}$ . Furthermore, if we choose  $\theta_3^* \stackrel{\text{def}}{=} \bar{\theta}_1$ , then the (theoretical) convergence rate is optimal and it is equal to  $\rho_3^* \stackrel{\text{def}}{=} 1 - \theta_3^*$ .

**Proof.** Since Algorithm 4.1 can be represented by (28), we need to show that  $\rho(G_3(\theta))$ , the spectral radius of  $G_3(\theta)$ , is less than 1. First, note that by Lemmas 4.3, 4.4 and 4.5, we have  $\rho(G_3(\theta)) = \rho_3(\theta)$ . Using Lemma 4.2 we conclude that the function  $\theta \mapsto \rho_3(\theta)$  is increasing on the interval  $[\bar{\theta}_1, \infty)$ , which means that its minimum is attained at  $\bar{\theta}_1$ . To finish the proof, it is enough to prove that  $\rho_3(\theta) = 1$  if and only if

$$\theta = \frac{2\sqrt{\lambda n}}{\sqrt{\lambda n} + \sigma_1}.$$

Note that

$$\begin{aligned} \rho_3(\theta) = 1 &\Leftrightarrow \theta \sigma_1 \sqrt{\delta_1(\theta)} + \theta^2 \sigma_1^2 - 2(1 - \theta)\lambda n = 2\lambda n \\ &\Rightarrow \theta^2 \sigma_1^2 \delta_1(\theta) = \left( 2(2 - \theta)\lambda n - \theta^2 \sigma_1^2 \right)^2 \\ &\Leftrightarrow \frac{2 - \theta}{\theta} = \frac{\sigma_1}{\sqrt{\lambda n}} \\ &\Leftrightarrow \theta = \frac{2\sqrt{\lambda n}}{\sqrt{\lambda n} + \sigma_1} \end{aligned}$$

and



$$\begin{aligned}\theta = \frac{2\sqrt{\lambda n}}{\sqrt{\lambda n} + \sigma_1} &\Leftrightarrow \theta^2 \sigma_1^2 = \lambda n (2 - \theta)^2 \\ &\Leftrightarrow \theta \sigma_1 \sqrt{\delta_1(\theta)} + \theta^2 \sigma_1^2 - 2(1 - \theta)\lambda n = 2\lambda n,\end{aligned}$$

completing the proof.  $\square$

It is worth noting that if the spectral radius of  $M_1$  is less than 1, that is, if  $\sigma_1^2 < \lambda n$ , then Algorithms 3.2, 3.3 and 4.1 converge for any choice of  $\theta \in (0, 1]$ . Indeed, in this case we have

$$\frac{2\lambda n}{\lambda n + \sigma_1^2} > \frac{2\sqrt{\lambda n}}{\sqrt{\lambda n} + \sigma_1} > 1,$$

which implies that the set of admissible values for  $\theta$  established in Theorems 3.4, 3.5 and 4.6 contains the whole interval  $(0, 1]$ .

On the other hand, if  $\sigma_1^2 \geq \lambda n$ , the convergence of these algorithms is more restrictive. Moreover, in this case we have

$$\frac{2\lambda n}{\lambda n + \sigma_1^2} \leq \frac{2\sqrt{\lambda n}}{\sqrt{\lambda n} + \sigma_1} \leq 1,$$

which means that Algorithm 4.1 has a broader range for  $\theta$  than Algorithms 3.2 and 3.3.

#### 4.2. Complexity results

Taking into account (22), (25), the relation  $\log(1 - \theta) \approx -\theta$  and Theorem 4.6, we conclude that the complexity of our Accelerated Fixed Point Method, Algorithm 4.1, is proportional to

$$\frac{1}{2\theta_3^*} = \frac{\sigma_1^2}{-4\lambda n + 4\sqrt{\lambda n(\lambda n + \sigma_1^2)}} \stackrel{(25)}{=} \frac{\kappa - \lambda n}{4(\sqrt{\lambda n \kappa} - \lambda n)}. \quad (35)$$

Note that in the case when  $\lambda = 1/n$ , as is typical in machine learning applications, we can write

$$\frac{1}{2\theta_3^*} \stackrel{(35)}{=} \frac{\kappa - 1}{4(\sqrt{\kappa} - 1)} = \frac{\sqrt{\kappa} + 1}{4}. \quad (36)$$

**This is very surprising as it means that we are achieving the optimal accelerated Nesterov rate  $\tilde{O}(\sqrt{\kappa})$ .**

## 5. Extensions

In this section we discuss some variants of Algorithm 4.1. The first one consists of switching the order of the computations, updating the dual variable first and then the primal one.

The second approach updates the primal variable enforcing the first relation of the optimality conditions given by (10) and using the relaxation parameter  $\theta$  only to update the dual variable.

### 5.1. Switching the update order

This approach updates the dual variable  $\alpha$  first and then updates the primal variable  $w$  using the new information about  $\alpha$ . This is summarized in the following scheme.

$$\begin{cases} \alpha^{k+1} = (1 - \theta)\alpha^k + \theta(y - A^T w^k) \\ w^{k+1} = (1 - \theta)w^k + \theta \frac{1}{\lambda n} A \alpha^{k+1}. \end{cases} \quad (37)$$

As we shall see now, this scheme provides the same complexity results as Algorithm 4.1. To see this, note that the iteration (37) is equivalent to

$$\begin{pmatrix} I & -\frac{\theta}{\lambda n} A \\ 0 & I \end{pmatrix} \begin{pmatrix} w^{k+1} \\ \alpha^{k+1} \end{pmatrix} = \begin{pmatrix} (1 - \theta)I & 0 \\ -\theta A^T & (1 - \theta)I \end{pmatrix} \begin{pmatrix} w^k \\ \alpha^k \end{pmatrix} + \begin{pmatrix} 0 \\ \theta y \end{pmatrix}$$

or in a compact way,

$$x^{k+1} = G(\theta)x^k + f$$

with

$$G(\theta) = (1 - \theta)I + \theta \begin{pmatrix} -\frac{\theta}{\lambda n} A A^T & \frac{1 - \theta}{\lambda n} A \\ -A^T & 0 \end{pmatrix}.$$

It can be shown that the matrix  $G(\theta)$  has exactly the same spectrum of  $G_3(\theta)$ , defined in (29). So, the convergence result is also the same, which we state again for convenience.

**Theorem 5.1.** *Let  $w^0 \in \mathbb{R}^d$  and  $\alpha^0 \in \mathbb{R}^N$  be arbitrary and consider the sequence  $(w^k, \alpha^k)_{k \in \mathbb{N}}$  defined by (37) with  $\theta \in \left(0, \frac{2\sqrt{\lambda n}}{\sqrt{\lambda n} + \sigma_1}\right)$ . Then the sequence  $(w^k, \alpha^k)$  converges to the (unique) solution of the problem (4) at an asymptotic linear rate of*

$$\rho_3(\theta) = \begin{cases} 1 - \theta, & \text{if } \theta \in (0, \bar{\theta}_1] \\ \frac{1}{2\lambda n} \left( \theta \sigma_1 \sqrt{\delta_1(\theta)} + \theta^2 \sigma_1^2 - 2(1 - \theta)\lambda n \right), & \text{if } \theta \geq \bar{\theta}_1, \end{cases}$$

where  $\bar{\theta}_1 = \frac{-2\lambda n + 2\sqrt{\lambda n(\lambda n + \sigma_1^2)}}{\sigma_1^2}$ . Furthermore, if we choose  $\theta_3^* = \bar{\theta}_1$ , then the (theoretical) convergence rate is optimal and it is equal to  $\rho_3^* = 1 - \theta_3^*$ .

## 5.2. Maintaining primal-dual relationship

The second approach updates the primal variable enforcing the first relation of the optimality conditions given by (10) and uses the relaxation parameter  $\theta$  only to update the dual variable, as described in the following scheme.

$$\begin{cases} w^{k+1} = \frac{1}{\lambda n} A \alpha^k \\ \alpha^{k+1} = (1 - \theta) \alpha^k + \theta (y - A^T w^{k+1}). \end{cases} \quad (38)$$

Differently from the previous case, this scheme cannot achieve accelerated convergence. Indeed, note first that the scheme (38) can be written as

$$\begin{pmatrix} I & 0 \\ \theta A^T & I \end{pmatrix} \begin{pmatrix} w^{k+1} \\ \alpha^{k+1} \end{pmatrix} = \begin{pmatrix} 0 & \frac{1}{\lambda n} A \\ 0 & (1 - \theta) I \end{pmatrix} \begin{pmatrix} w^k \\ \alpha^k \end{pmatrix} + \begin{pmatrix} 0 \\ \theta y \end{pmatrix}$$

or in a compact way,

$$x^{k+1} = G(\theta) x^k + f$$

with

$$G(\theta) = \begin{pmatrix} 0 & \frac{1}{\lambda n} A \\ 0 & (1 - \theta) I - \frac{\theta}{\lambda n} A^T A \end{pmatrix}.$$

We can conclude that the eigenvalues of this matrix are

$$\left\{ 1 - \theta - \frac{\theta \sigma_j^2}{\lambda n}, j = 1, \dots, p \right\} \cup \{1 - \theta\},$$

exactly the same of the matrix  $G_1(\theta)$ , the iteration matrix of Algorithm 3.1 with employment of  $M_1$ . So, the complexity analysis here is the same as that one established in Theorem 3.4.

## 5.3. Maintaining primal-dual relationship 2

For the sake of completeness, we present next the method where we keep the second relationship intact and include  $\theta$  in the first relationship. This leads to

$$\begin{cases} \alpha^{k+1} = y - A^T w^k \\ w^{k+1} = (1 - \theta)w^k + \frac{\theta}{\lambda n} A \alpha^{k+1}. \end{cases} \quad (39)$$

Here we obtain the same convergence results as the ones described in Section 5.2. In fact, the relations above can be written as

$$\begin{pmatrix} 0 & I \\ I & -\frac{\theta}{\lambda n} A \end{pmatrix} \begin{pmatrix} w^{k+1} \\ \alpha^{k+1} \end{pmatrix} = \begin{pmatrix} -A^T & 0 \\ (1 - \theta)I & 0 \end{pmatrix} \begin{pmatrix} w^k \\ \alpha^k \end{pmatrix} + \begin{pmatrix} y \\ 0 \end{pmatrix}$$

or in a compact way,  $x^{k+1} = G(\theta)x^k + f$  with

$$G(\theta) = \begin{pmatrix} (1 - \theta)I - \frac{\theta}{\lambda n} A A^T & 0 \\ -A^T & 0 \end{pmatrix}.$$

We can conclude that the eigenvalues of this matrix are

$$\left\{ 1 - \theta - \frac{\theta \sigma_j^2}{\lambda n}, j = 1, \dots, p \right\} \cup \{1 - \theta\},$$

exactly the same of the matrix  $G_1(\theta)$ , the iteration matrix of Algorithm 3.1 with employment of  $M_1$ . So, the complexity analysis here is the same as that one established in Theorem 3.4.

Observe that in (38) we have

$$w^{k+1} = \phi_1(\alpha^k) \quad \text{and} \quad \alpha^{k+1} = \phi_2(\theta, \alpha^k, w^{k+1}).$$

On the other hand, in (39) we have

$$\alpha^{k+1} = \phi_3(w^k) \quad \text{and} \quad w^{k+1} = \phi_4(\theta, w^k, \alpha^{k+1}).$$

It is worth noting that if we update the variables as

$$\alpha^{k+1} = \phi_2(\theta, \alpha^k, w^k) \quad \text{and} \quad w^{k+1} = \phi_1(\alpha^{k+1})$$

or

$$w^{k+1} = \phi_4(\theta, w^k, \alpha^k) \quad \text{and} \quad \alpha^{k+1} = \phi_3(w^{k+1})$$

we obtain

$$\begin{pmatrix} -\frac{\theta}{\lambda n} A A^T & \frac{(1-\theta)}{\lambda n} A \\ -\theta A^T & (1 - \theta)I \end{pmatrix} \quad \text{and} \quad \begin{pmatrix} (1 - \theta)I & \frac{\theta}{\lambda n} A \\ -(1 - \theta)A^T & -\frac{\theta}{\lambda n} A^T A \end{pmatrix}$$

**Table 2**

Comparison between the ranges of  $\theta$  to ensure convergence, optimal convergence rates, complexity and cost per iteration (# of arithmetic operations) of the algorithms proposed in this paper: Algorithm 3.2, indicated by PDFP1( $\theta$ ); Algorithm 3.3, denoted by PDFP2( $\theta$ ); Algorithm 4.1, QTZ( $\theta$ ) and the extensions (37) (New Quartz) and (38) (Modified Quartz), indicated by NQTZ( $\theta$ ) and MQTZ( $\theta$ ), respectively.

	Range of $\theta$	Optimal rate	Complexity	Cost/iteration
PDFP1( $\theta$ )	$\left(0, \frac{2\lambda n}{\lambda n + \sigma_1^2}\right)$	$\frac{\sigma_1^2}{2\lambda n + \sigma_1^2}$	(26)	$10dN + 5d + 9N$
PDFP2( $\theta$ )	$\left(0, \frac{2\lambda n}{\lambda n + \sigma_1^2}\right)$	$\sqrt{\frac{\sigma_1^2}{\lambda n + \sigma_1^2}}$	(27)	$6dN + 5d + 9N$
QTZ( $\theta$ )	$\left(0, \frac{2\sqrt{\lambda n}}{\sqrt{\lambda n} + \sigma_1}\right)$	$1 - \theta_3^*$	(36)	$6dN + 5d + 9N$
NQTZ( $\theta$ )	$\left(0, \frac{2\sqrt{\lambda n}}{\sqrt{\lambda n} + \sigma_1}\right)$	$1 - \theta_3^*$	(36)	$6dN + 5d + 9N$
MQTZ( $\theta$ )	$\left(0, \frac{2\lambda n}{\lambda n + \sigma_1^2}\right)$	$\frac{\sigma_1^2}{2\lambda n + \sigma_1^2}$	(26)	$6dN + 3d + 9N$

as the associated iteration matrices, respectively. Moreover, we can conclude that they also have the same spectrum of  $G_1(\theta)$ . So, the complexity analysis is the same as that one established in Theorem 3.4.

## 6. Numerical experiments

In this section we present a comparison among the methods discussed in this work. Besides a table with the convergence rates and complexity bounds, we show here some numerical tests performed to illustrate the properties of Algorithms 3.2, 3.2 and 4.1 as well as of the extensions (37) and (38) applied to solve the primal-dual ridge regression problem stated in (4). We refer to Algorithm 4.1 as Quartz and the extensions (37) and (38) as New Quartz and Modified Quartz, respectively. The name Quartz is due to the fact that Algorithm 4.1 is a deterministic version of a randomized primal-dual algorithm proposed and analyzed by Qu, Richtárik and Zhang [7].

We summarize the main features of these methods in Table 2 which brings the range of the parameter to ensure convergence, the optimal convergence rates, the complexity and the cost per iteration of each method. For instance, the two versions of Algorithm 3.1 have the same range for theta. The usage of  $M_1$  provides best convergence rate compared with using  $M_2$ . However, it requires more calculations per iteration: the major computational tasks to be performed are computation of the matrix–vector products  $AA^T w$  and  $A^T A \alpha$ , while the use of  $M_2$  needs the computation of  $A \alpha$  and  $A^T w$ .

Surprisingly, Algorithm 4.1 has shown to be the best from both the theoretical point of view and the numerical experiments and with the same cost as the computation of  $A \alpha$  and  $A^T w$ .

We also point out that the modified Quartz, (38), did not have here the same performance as the randomized version studied in [7].

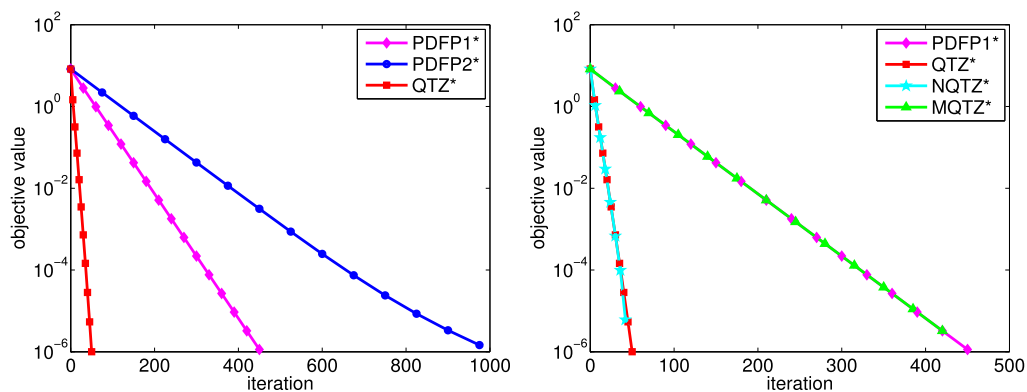
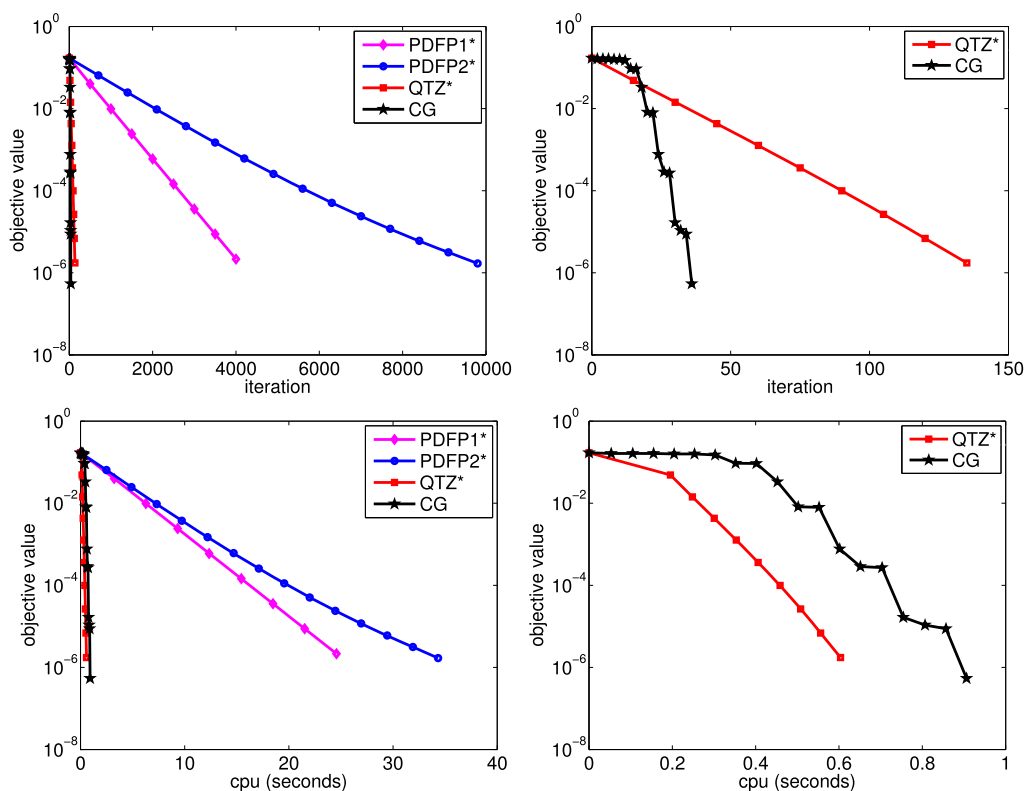


Fig. 7. Performance of the optimal versions of the algorithms proposed in this paper applied to solve the problem (4). The pictures show the objective values against the number of iterations. The dimensions considered were  $d = 10$ ,  $m = 1$  and  $n = 500$ . The matrix  $A \in \mathbb{R}^{d \times N}$  and the vector  $y \in \mathbb{R}^N$  were randomly generated. For simplicity of notation we have denoted Algorithm 3.2 by PDFP1\*, Algorithm 3.3 by PDFP2\*, Algorithm 4.1 by QTZ\* and the extensions (37) (New Quartz) and (38) (Modified Quartz) by NQTZ\* and MQTZ\*, respectively. In order to keep the figure legible, we plotted a diamond every 30 iterations for PDFP1\*, a circle every 75 iterations for PDFP2\*, a square every 5 iterations for QTZ\*, a star every 6 iterations for NQTZ\* and a triangle every 35 iterations for MQTZ\*.

Fig. 7 illustrates these features, showing the primal-dual objective values against the number of iterations. The dimensions considered were  $d = 10$ ,  $m = 1$  and  $n = 500$ . We adopted the optimal parameters associated with each method, namely,  $\theta_1^*$ ,  $\theta_2^*$  and  $\theta_3^*$  for Algorithms 3.2, 3.3 and 4.1, respectively,  $\theta_3^*$  for the algorithm given by (37) and  $\theta_1^*$  for the algorithm given by (38). These parameters are defined in Theorems 3.4, 3.5 and 4.6 and the computational cost of computing them is the same as the cost of computing  $\sigma_1$ , the largest singular value of  $A$ .

The left picture of Fig. 7 compares Algorithms 3.2, 3.3 and 4.1, while the right one shows the performance of Algorithm 3.2 and the three variants of Quartz. We can see the equivalence between Quartz and New Quartz and also the equivalence between Modified Quartz and Algorithm 3.2. Note that, besides the advantage of QTZ\* in terms of number of iterations, it does not need more arithmetic operations per iteration as we have seen in Table 2.

Despite the main goal of this work being a theoretical study about convergence and complexity of various fixed point type methods, for the sake of completeness, we present here a comparison of our methods with the classical one for solving quadratic optimization problems: the conjugate gradient algorithm (CG). Fig. 8 shows the performance of the optimal versions of the algorithms proposed in this paper compared with CG, applied to solve the problem (4). On the top we have plotted the objective values against the number of iterations, while the bottom pictures show the objective values against the cpu time. The numerical experiments indicate that Quartz is competitive with CG. While Quartz needs more iterations than CG to converge, it is faster in runtime. This is due to the big difference between the effort per iteration of these two algorithms:  $6dN + 5d + 9N$  arithmetic operations per iteration for Quartz compared to  $4d^2 + 4N^2 + 4dN + 14d + 17N$



**Fig. 8.** Performance of the optimal versions of the algorithms proposed in this paper compared with the conjugate gradient algorithm, applied to solve the problem (4). The dimensions considered were  $d = 200$ ,  $m = 1$  and  $n = 5000$ . The matrix  $A \in \mathbb{R}^{d \times N}$  and the vector  $y \in \mathbb{R}^N$  were randomly generated. For simplicity of notation we have denoted Algorithm 3.2 by PDFP1\*, Algorithm 3.3 by PDFP2\*, Algorithm 4.1 by QTZ\* and conjugate gradient by CG. The pictures on the top show the objective values against the number of iterations, while the bottom ones show the objective values against the cpu time. The right pictures present the results of QTZ\* and CG of the left ones with the horizontal axis rescaled. For ease of presentation, we plotted a diamond every 500 iterations for PDFP1\*, a circle every 700 iterations for PDFP2\*, a square every 15 iterations for QTZ\* and a star every 2 iterations for CG. Note that despite QTZ\* spent more iterations than CG, the computational time for solving the problem was less than that for CG. We stress that before starting to compute the iterates of PDFP1\*, PDFP2\* and QTZ\*, we need to compute the optimal parameters  $\theta_1^*$ ,  $\theta_2^*$  and  $\theta_3^*$ , which have the same computational cost as the cost of computing  $\sigma_1$ , the largest singular value of  $A$ . The time spent computing  $\sigma_1$  was taken into account and we can see this more clearly in the bottom right plot.

for CG. It should be noted, however, that Quartz requires a pre-computation in order to obtain  $\sigma_1$ . Fortunately, the number of operations required to calculate  $\sigma_1$  is  $O(dN)$ , as established in [17].

## 7. Conclusion

In this paper we have proposed and analyzed several algorithms for solving the ridge regression problem and its dual. We have developed a (parameterized) family of fixed point methods applied to various equivalent reformulations of the optimality conditions.

We have performed a convergence analysis and obtained complexity results for these methods, revealing interesting geometrical insights between convergence speed and spectral properties of iteration matrices. Our main method achieves the optimal accelerated rate of Nesterov. We have performed some numerical experiments to illustrate the properties of our algorithms as well as a comparison with the conjugate gradient algorithm. The numerical experiments indicate that our main algorithm is competitive with the conjugate gradient algorithm.

## References

- [1] Y. Saad, *Iterative Methods for Sparse Linear Systems*, SIAM, 2003.
- [2] S. Shalev-Shwartz, T. Zhang, Stochastic dual coordinate ascent methods for regularized loss, *J. Mach. Learn. Res.* 14 (1) (2013) 567–599.
- [3] S. Shalev-Shwartz, T. Zhang, Accelerated proximal stochastic dual coordinate ascent for regularized loss minimization, *Math. Program., Ser. A* 155 (2016) 105–145.
- [4] T. Zhang, On the dual formulation of regularized linear systems with convex risks, *Mach. Learn.* 46 (1) (2002) 91–129.
- [5] A. Chambolle, T. Pock, A first-order primal-dual algorithm for convex problems with applications to imaging, *J. Math. Imaging Vision* 40 (2011) 120–145.
- [6] N. Komodakis, J.C. Pesquet, Playing with duality: an overview of recent primal-dual approaches for solving large-scale optimization problems, *IEEE Signal Process. Mag.* 32 (6) (2015) 31–54.
- [7] Z. Qu, P. Richtárik, T. Zhang, Quartz: randomized dual coordinate ascent with arbitrary sampling, in: *Adv. Neural Inf. Process. Syst.*, vol. 28, 2015, pp. 865–873.
- [8] K.J. Arrow, L. Hurwicz, Gradient method for concave programming I: local results, in: K.J. Arrow, L. Hurwicz, H. Uzawa (Eds.), *Studies in Linear and Nonlinear Programming*, Stanford University Press, Stanford, 1958, pp. 117–126.
- [9] H. Uzawa, Iterative methods for concave programming, in: K.J. Arrow, L. Hurwicz, H. Uzawa (Eds.), *Studies in Linear and Nonlinear Programming*, Stanford University Press, Stanford, 1958, pp. 117–126.
- [10] A.E. Hoerl, Application of ridge analysis to regression problems, *Chem. Eng. Prog.* 58 (1962) 54–59.
- [11] A.E. Hoerl, R.W. Kennard, Ridge regression: biased estimation for nonorthogonal problems, *Technometrics* 12 (1) (1970) 55–67.
- [12] M. El-Dereny, N.I. Rashwan, Solving multicollinearity problem using ridge regression models, *Int. J. Contemp. Math. Sci.* 6 (2011) 585–600.
- [13] D.M. Hawkins, X. Yin, A faster algorithm for ridge regression of reduced rank data, *Comput. Statist. Data Anal.* 40 (2) (2002) 253–262.
- [14] C. Saunders, A. Gammerman, V. Vovk, Ridge regression learning algorithm in dual variables, in: *Proceedings of the 15th International Conference on Machine Learning*, Morgan Kaufmann Publishers Inc., 1998, pp. 515–521.
- [15] H.D. Vinod, A survey of ridge regression and related techniques for improvements over ordinary least squares, *Rev. Econ. Stat.* 60 (1) (1978) 121–131.
- [16] T.C. Silva, A.A. Ribeiro, G.A. Peričaro, A new accelerated algorithm for ill-conditioned ridge regression problems, *Comput. Appl. Math.* 37 (2) (2018) 1941–1958.
- [17] M. Brand, Fast low-rank modifications of the thin singular value decomposition, *Linear Algebra Appl.* 415 (1) (2006) 20–30.